

Electron Spin Resonance Study on Dynamic Heterogeneity in Miscible Blend of Poly(cyclohexyl methacrylate) and Poly(cyclohexyl acrylate)

Yohei Miwa,[†] Yusuke Sugino,[†] Katsuhiro Yamamoto,[†] Takuya Tanabe,[†] Masato Sakaguchi,[‡] Masahiro Sakai,[§] and Shigetaka Shimada^{*,†}

Department of Materials Science & Engineering, Nagoya Institute of Technology, Gokiso-cho, Showa-ku, Nagoya 466-8555, Japan; Nagoya Keizai University, 61 Uchikubo, Inuyama, 484-8503, Japan; and Research Center for Molecular-Scale Nanoscience, Institute for Molecular Science, 38 Nishigo-Naka, Myodaiji, Okazaki 444-8585, Japan

Received May 18, 2004; Revised Manuscript Received June 3, 2004

ABSTRACT: Electron spin resonance (ESR) was applied to estimate the segmental dynamics of poly(cyclohexyl methacrylate) (PCHMA) and poly(cyclohexyl acrylate) (PCHA) in their miscible blend. The PCHMA and PCHA chains were labeled with nitroxide radicals, and the temperature-dependent ESR spectra of the spin-labels selectively reflected the segmental dynamics of the labeled chains in the blend. The ESR result showed different mobility between PCHMA and PCHA chains even though their blend showed a single glass transition in any composition by a calorimetric measurement. The WLF treatment demonstrated that a transition temperature, $T_{5.0\text{mT}}$, at which the extreme separation width due to ^{14}N anisotropic hyperfine splitting was 5.0 mT, reflected the glass transition observed at a frequency of the ESR. The $T_{5.0\text{mT}}$ of poly(CHMA-*random*-CHA) was dependent on the composition; namely, the mobility of the spin-labels was sensitive to the composition around them. The self-concentration model suggested by Lodge and McLeish [Lodge, T. P.; McLeish, T. C. B. *Macromolecules* 2000, 33, 5278] was used to interpret the segmental dynamics of the PCHMA and PCHA in the blend estimated by the ESR. The Lodge–McLeish model provided the excellent prediction of the segmental dynamics of the PCHMA in the blend. The segmental dynamics of the PCHA chain in the blend was also explained well by the Lodge–McLeish model although the experimental values were slightly higher than the predicted ones. The mobility of the nitroxides labeled to the PCHA chains might be restricted by the rigid PCHMA component in the blend. These results imply that the dimension of a region observed by the ESR method is comparable to the cube of the Kuhn length suggested by Lodge and McLeish.

Introduction

Spin-probes and spin-labels have been widely used to obtain information about relaxation process in polymers. The ESR spectrum of the nitroxide radical is a function of its rotational motion and is sensitive to the mobility of the nitroxide. It is well-known that the mobility of the nitroxide radicals is related to the dynamics of the host polymer.^{1–12} The spin-label technique is useful to detect molecular mobility and environments in particular sites or regions of host polymers. Recently, the spin-label technique was applied to detect the local molecular mobility in homopolymers, block copolymer, and random copolymer, for instance, the chain ends, interfacial region of the microphase separations of diblock copolymers, etc.^{4–7} The mobility of the nitroxides labeled to random copolymers was dependent on the composition.⁵ This result indicates that the mobility of the nitroxides is sensitive to the composition around them.

Recently, the viscoelastic properties of miscible polymer blends have been the focus of study.^{13–29} Some experimental techniques (NMR,^{20,27,30} dielectric spectroscopy,^{15,16,23,30,31} quasielastic neutron scattering,³² ESR,^{33,34} mechanical measurements,^{25,26} etc.) provided the evidence of thermorheological complexity, which is defined as the failure of the empirical time–temperature superposition principle in describing system dy-

namics. It appears that the two components maintain their own dynamic identities even though the blend is thermodynamically miscible. To interpret these experimental results, concentration fluctuations (driven by the thermodynamics of the blends)^{15,28,29} and a self-concentration effect induced by the chain connectivity^{19,20,24} were mainly used. Recently, Leroy et al. proposed a model that took into account the both effects, the self-concentration and the concentration fluctuation, and the model agreed well with their experimental results.¹⁶ Their model basically took the idea of an effective concentration for a given polymer segment in the blend and, in addition, assumed a distribution of effective concentrations mainly due to the segmental dynamics of a given component, the corresponding Kuhn length. Kant et al. estimated the temperature dependence of the both effects (the concentration fluctuation and the self-concentration) and the size of a cooperative volume.¹³ Since the concentration fluctuation played a minor role in determining the mean segmental relaxation times of the blend components at high temperatures (ca. $T_g + 50$ K), they concluded that the self-concentration effect induced by the chain connectivity provided a good description of the mean segmental dynamics in the temperature range. The results of Leroy et al. and Kant et al. agreed well with each other.

Siol et al. reported that the poly(cyclohexyl methacrylate) (PCHMA) and poly(cyclohexyl acrylate) (PCHA) were a compatible pair above 293 K (upper critical solution temperature, UCST).³⁵ Our calorimetric analysis also provided that the PCHMA and PCHA were mixing with each other (see Figure 2). This is the first

[†] Nagoya Institute of Technology.

[‡] Nagoya Keizai University.

[§] Institute for Molecular Science.

* Corresponding author: E-mail shimada.shigetaka@nitech.ac.jp.

study on the dynamics heterogeneity in this blend. As described above, the mobility of the spin-labels is influenced by the composition around them. Namely, the effective composition and mobility around each component in the PCHMA/PCHA blend will be probed through motional changes of the ESR spectra of the labels. In this paper, the local dynamic environments experienced by the each component in the miscible PCHMA/PCHA blend were examined by the ESR spin-label technique.

Experimental Section

Materials. Inhibitors in cyclohexyl methacrylate (CHMA, Extra Pure Reagent, Tokyo Chemical Co., Ltd.), cyclohexyl acrylate (CHA, Extra Pure Reagent, Kishida Chemical Co., Ltd.), *tert*-butyl methacrylate (*t*BMA, Extra Pure Reagent, Tokyo Chemical Co., Ltd.), and *tert*-butyl acrylate (*t*BA, Extra Pure Reagent, Tokyo Chemical Co., Ltd.) were adsorbed on activate aluminum oxide (particle size 2–4 mm, Kanto Chemical Co., Inc.) and removed. Benzoyl peroxide (BPO, Reagent, Nacalai Tesque Co., Ltd.) and 2,2,6,6-tetramethyl-4-aminopiperidine-1-oxyl (4-amino-TEMPO, 99%, Aldrich) were used as received. Tetrahydrofuran (THF, Extra Pure Reagent, Nacalai Tesque) were distilled under reduced pressure. Toluene and methanol (Extra Pure Reagent) were obtained from Nacalai Tesque and used without further purification.

Sample Synthesis and Selective Spin-Labeling. Poly(CHMA-*random-t*BMA) and poly(CHA-*random-t*BA) were polymerized by radical polymerization initiated by BPO. The polymerization was carried out in a vacuum condition at 363 K. The initial molar compositions of *t*BMA and *t*BA were 1 mol % against the CHMA and CHA, respectively. As a result, some *tert*-butyl moieties were randomly incorporated into the PCHMA and PCHA chains. The reaction mixture was dissolved into toluene and precipitated into excess methanol. After a filtration, the samples were dried in a vacuum at 343 K for 24 h. For spin-labeling, an amide–ester interchange reaction between the *tert*-butyl moiety and 4-amino-TEMPO was carried out in toluene at 283 K for 4 days. The spin-labeled PCHMA and PCHA were precipitated from toluene solution to excess methanol, filtered to remove a large amount of unreacted spin-label reagents, and finally dried in a vacuum at 393 K for 24 h. This precipitation was repeated more than four times to completely remove the unreacted spin-label reagents. The chemical structures of the spin-labeled PCHMA and PCHA are shown in Figure 1.

The random copolymerizations of the CHMA and CHA with various compositions were carried out using the BPO as an initiator in a vacuum condition at 363 K. 1 mol % of the *t*BA was added to the reaction mixture before the copolymerization, and some *tert*-butyl moieties were randomly incorporated into a poly(CHMA-*random*-CHA) chain. The spin-label and purification were carried out as described above. Compositions of the poly(CHMA-*random*-CHA)s were determined by nuclear magnetic resonance (NMR).

The number-averaged molecular weight (M_n) and its distribution (M_w/M_n) of the all samples were determined by gel permeation chromatography (GPC) using PS standards (Tosoh). The M_n 's and M_w/M_n 's of the PCHMA and PCHA were 150K and 2.7 and 22K and 6.9, respectively.

Preparation of Blend Samples. PCHMA/PCHA blend samples were prepared as follows. First, PCHMA and PCHA were dissolved in THF to make 10 wt % solution and mixed with each other. The mixed solution was dried on a Teflon plate at 313 K. After the films were dried for 2 days, the films were annealed in a vacuum at 413 K for 24 h.

Measurement. GPC was carried out with following condition: in THF (1 mL/min) at 313 K on four polystyrene gel columns (Tosoh TSK gel GMH (beads size is 7 μ m), G4000H, G2000H, and G1000H (5 μ m)) that were connected to a Tosoh CCPE (Tosoh) pump and an ERC-7522 RI refractive index detector (ERMA Inc.). The columns were calibrated against standard PS (Tosoh) samples.

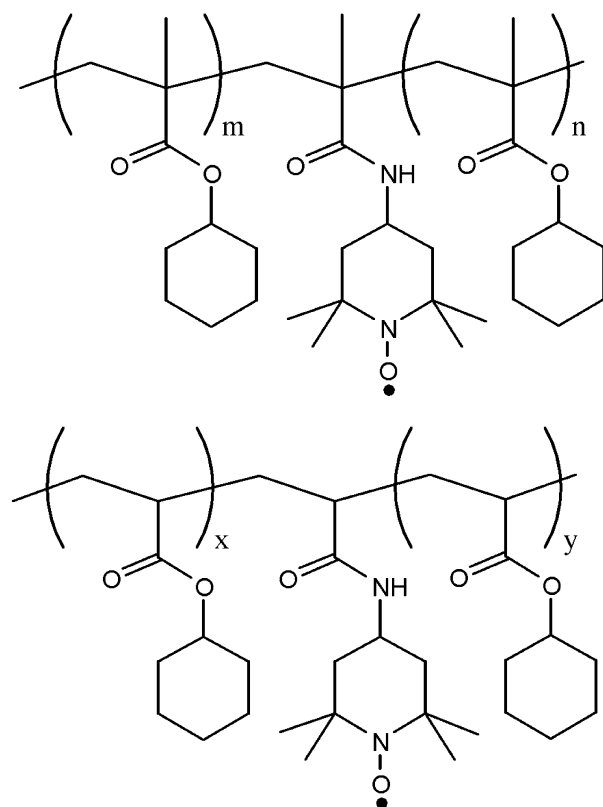


Figure 1. Chemical structures of spin-labeled PCHMA (top) and PCHA (bottom).

NMR was performed on a Bruker AVANCE 200 spectrometer using deuterated chloroform at 298 K with tetramethylsilane as an internal reference.

Each sample was contained in a quartz tube, and the tube was depressurized to a pressure of 10^{-4} Torr and sealed before ESR measurement. ESR spectra at 77 K and higher temperatures were observed at low microwave power level to avoid power saturation and with 100 kHz fielded modulation using JEOL JES-FE3XG and JES-RE1XG spectrometers (X band) coupled to microcomputers (NEC PC-9801). The signal of 1,1-diphenyl-2-picrylhydrazyl (DPPH) was used as a g tensor standard. The magnetic field was calibrated with the well-known splitting constants of Mn^{2+} .

Differential scanning calorimetry (DSC, MDSC 2920) manufactured by TA Instruments was used. Samples were heated from a room temperature to ca. $T_g + 100$ K at a rate of 20 K/min, kept for 5 min, and cooled at a rate of 10 K/min. The data collection was carried out on the cooling process. The calorimeter was calibrated with an indium standard.

Results and Discussion

1. Broad Single Glass Transition of PCHMA/PCHA Blends in DSC Measurement. DSC traces of the PCHMA/PCHA blends on the cooling at a rate of 10 K/min are shown in Figure 2b. All PCHMA/PCHA blends with different compositions showed single glass transitions. This demonstrates that the compatible mixing of the both components in the molecular order. The DSC traces of the heating process of the blend also showed the single glass transitions. The T_g was taken to be the midpoint, i.e., the temperature corresponding to half of the endothermic shift, and included ± 2 K of experimental errors. The T_g of the PCHMA/PCHA blend was plotted against the weight fraction of PCHA component (ϕ_{PCHA}) in Figure 2a. The T_g of the PCHMA/PCHA blend was fitted well by the Gordon–Taylor

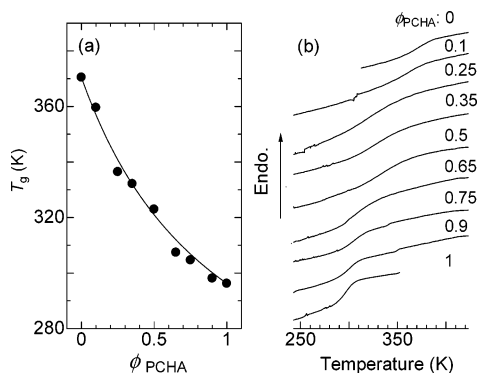


Figure 2. (a) Plots of T_g of PCHMA, PCHA, and blends as a function of ϕ_{PCHA} . The solid curve is presented by the Gordon–Taylor equation with $K = 0.5$. (b) DSC traces.

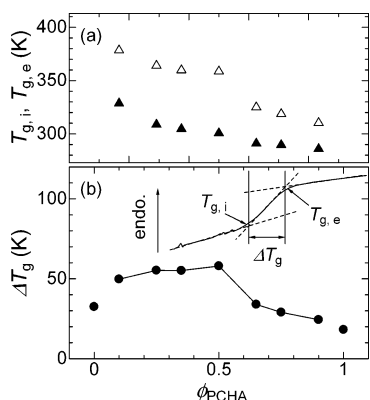


Figure 3. (a) Plots of $T_{g,i}$ (solid) and $T_{g,e}$ (open) against ϕ_{PCHA} . (b) Plots of ΔT_g against ϕ_{PCHA} . The definitions of $T_{g,i}$, $T_{g,e}$, and ΔT_g are shown in the figure.

equation. The Gordon–Taylor equation is given by³⁶

$$T_g = (T_{g,\text{PCHA}}\phi_{\text{PCHA}} + KT_{g,\text{PCHMA}}(1 - \phi_{\text{PCHA}})) / (\phi_{\text{PCHA}} + K(1 - \phi_{\text{PCHA}})) \quad (1)$$

where $T_{g,\text{PCHA}}$ and $T_{g,\text{PCHMA}}$ are the glass transition temperatures of the PCHA and PCHMA homopolymers, respectively. K is a fitting parameter to be 0.5 for the PCHMA/PCHA blend. The K smaller than unity implies a weak interaction between the PCHMA and PCHA chains.

The broadness of the glass transitions (ΔT_g), $T_{g,i}$, and $T_{g,e}$ of both homopolymers and PCHMA/PCHA blends were plotted as a function of the ϕ_{PCHA} in Figure 3. The ΔT_g , $T_{g,i}$, and $T_{g,e}$ were defined as shown in the figure. The blending increased the ΔT_g . This implies that the distributions of the τ_c of the α relaxation process in the samples increased with an increase in heterogeneity of the segmental concentration. The highest value of the ΔT_g was observed around $\phi_{\text{PCHA}} = 0.5$. It is interesting that the ΔT_g 's of the PCHMA/PCHA blends with the major component of the PCHMA are larger than those of the PCHMA/PCHA blends with major components of the PCHA. Lodge and McLeish showed the simulated DSC traces based on the self-concentration induced by the chain connectivity, when it was assumed that the calorimetric T_g reflects the different local environments between the samples.²⁴ They insisted that the glass transitions of miscible blends are broader than those of the pure components, and the glass transition of a 25:75 blend is broader than a 75:25 blend of the same components (the lower T_g component listed first). Our

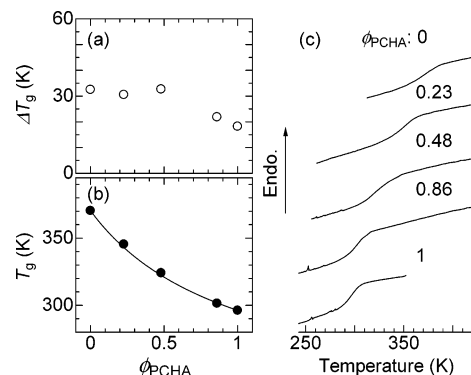


Figure 4. (a) Plots of ΔT_g of PCHMA, PCHA, and poly(CHMA-*random*-CHA) as a function of ϕ_{PCHA} . (b) Plots of T_g as a function of ϕ_{PCHA} . The curve is presented by the Gordon–Taylor equation with $K = 0.5$. (c) DSC traces.

experimental result is in good agreement with the calculation by Lodge and McLeish. This might imply that the PCHMA and PCHA had different dynamics induced by the self-concentration effect in the blend, and the difference of the mobility between the PCHMA and PCHA might be large when the PCHMA was the major component. Not only our DSC results but also that of other authors showed the same behavior.^{20,37}

The poly(CHMA-*random*-CHA) showed a single glass transition on the DSC trace (Figure 4c) due to the random distribution of the CHMA and CHA units along the chain. The T_g 's of the PCHMA, PCHA, and poly(CHMA-*random*-CHA) were plotted against the weight fraction of the ϕ_{PCHA} in Figure 4b. The composition-dependent T_g of the poly(CHMA-*random*-CHA) is also fitted with the eq 1 using the parameter K of 0.5. The K 's of the miscible polymer blend and random copolymer are sometimes different due to the different sequence of the monomeric units in the chain.³⁸ However, the K 's of the PCHMA/PCHA blend and poly(CHMA-*random*-CHA) were the same value. Factors determining T_g of the random copolymer can be considered to be compatible with those of the blend. In contrast with the obvious increase in the ΔT_g induced by blending of the PCHMA/PCHA, the ΔT_g of the poly(CHMA-*random*-CHA) is almost unchanged in comparison with those of the PCHMA and PCHA homopolymers. This is considered to indicate that local heterogeneity in the random copolymer is smaller than that in the blend because the random sequence of the CHMA and CHA units gives no self-concentration effect.

2. Estimation of Dynamic Heterogeneity in Miscible Blend by the Spin-Label Technique. 2.1. Molecular Mobility of PCHMA, PCHA, and Poly(CHMA-*random*-CHA). Temperature-dependent ESR spectra of the spin-labeled PCHMA and PCHA homopolymers and poly(CHMA-*random*-CHA) ($\phi_{\text{PCHA}} = 0.48$) are compared in the range 77–450 K (Figure 5). The temperature dependence of the spectra is brought from changes of the τ_c of the spin-labels. The outermost splitting width of main triplet spectrum induced by hyperfine coupling of the nitrogen nucleus narrows with an increase in mobility of the radicals because of motional averaging of the anisotropic interaction between an electron and the nucleus. The complete averaging gives rise to the isotropic narrowed spectrum. The isotropic narrowed spectrum was not observed for the PCHMA in this temperature range because of the high viscosity.

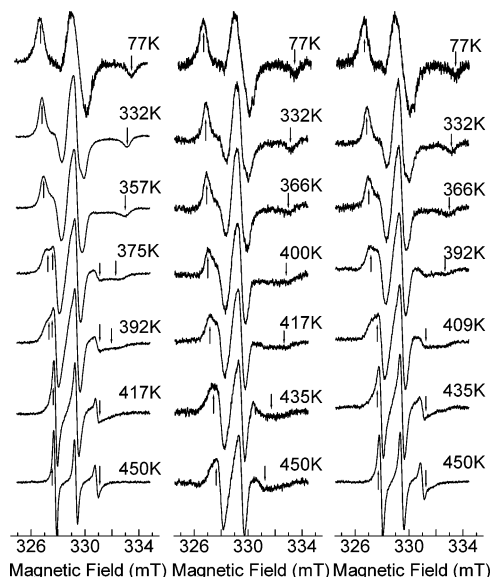


Figure 5. Comparison of temperature-dependent ESR spectra of spin-labeled PCHA (left), PCHMA (center), and poly(CHMA-random-CHA) ($\phi_{\text{PCHA}} = 0.48$) (right). Separation between arrows shows extreme separation width.

The superposition of two spectral components, a “first” and a “slow” component, was observed for a certain temperature range of the ESR spectra of the PCHA. The slow component with large outermost splitting width and the fast component with small outermost splitting width and narrow line width are considered to be attributed to radicals in rigid and mobile regions, respectively. On the other hand, the spectra comprising two components were not observed for the ESR spectra of the PCHMA and poly(CHMA-random-CHA). Typically, the two spectral components are observed for some semicrystalline polymers, immiscible polymer blends, block and graft copolymers, etc.,^{2,3,5,6,12,39–44} and those are not observed for amorphous homopolymers^{4,7} and random copolymers.⁵ It is considered that the two spectral components are the reflection of the heterogeneity of the τ_c of the spin-labels. It is hard to estimate the τ_c distribution from only the line shape of the ESR spectrum because not only a bimodal distribution but also a broad continuous distribution of the τ_c around the labels brings the two spectral components.⁴⁵ However, the mobility of the spin-labels reflected the glass transition of the PCHA (discussed below), and glass transitions of homopolymers are generally continuous. Therefore, we consider that the broad continuous distribution of the τ_c is the cause of the two spectral components of the PCHA.

A temperature dependence of the extreme separation width between arrows in Figure 5 is shown in Figure 6. The extreme separation width gradually decreases and steeply drops with an increase in temperature. A micro-Brownian-type molecular motion is considered to be the cause of the steep drop.^{4,7,46–48} $T_{5.0\text{mT}}$, at which the extreme separation width is equal to 5.0 mT, was estimated as a transition temperature of the molecular motion. The $T_{5.0\text{mT}}$'s of the PCHMA, PCHA, and poly(CHMA-random-CHA) are 428, 379, and 393 K, respectively. The $T_{5.0\text{mT}}$ includes an experimental uncertainty of ± 2.5 K. The $T_{5.0\text{mT}}$ appears at higher temperature than the T_g of the samples determined by the DSC because of a high frequency of the ESR.^{4,7,46–48} Recently, we estimated the difference between the $T_{5.0\text{mT}}$ and T_g

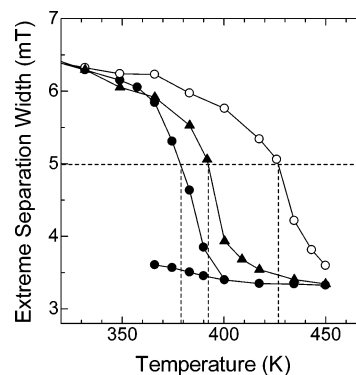


Figure 6. Temperature-dependent extreme separation width of ESR spectra of PCHMA (open circle), PCHA (solid circle), and poly(CHMA-random-CHA) ($\phi_{\text{PCHA}} = 0.48$) (triangle) shown in Figure 5.

of polystyrene (PS) and poly(methyl methacrylate) (PMMA) in detail using the time–temperature superposition, and it was found that the $T_{5.0\text{mT}}$ reflected the glass transition of the host polymers.^{4,7} The Williams–Landel–Ferry (WLF) equation is the successful relationship of temperature dependence for the viscoelastic response of polymers.⁴⁹

$$\log a_T = \log(\tau(T)/\tau(T_0)) = -C_1(T - T_0)/(C_2 + T - T_0) \quad (2)$$

where a_T is called the shift factor, τ is a relaxation time, T_0 is the chosen reference temperature, and C_1 and C_2 are constants. When T_0 is chosen to be T_g , the constants C_1^g and C_2^g are universal values of 17.44 and 51.6, respectively. The relaxation times of 7×10^{-9} s⁵⁰ and 100 s^{51,52} were substituted in $\tau(T)$ and $\tau(T_0)$, respectively. The $\Delta T (= T_{5.0\text{mT}} - T_g)$ was calculated to be 72 K from eq 2. On the other hand, ΔT obtained from the experiments was 58 and 83 K for the PCHMA and PCHA homopolymers, respectively. These experimental ΔT 's are in good agreement with the calculated one. The differences between the experimental and calculated ΔT 's are considered to be caused by the ambiguity of the C_1 and C_2 in the WLF equation. Anyhow, the experimental ΔT was explained well by the time–temperature superposition. Here, note that the spin-label used in this work is connected to the side group. However, the size of the spin-label is comparable with those of the CHMA and CHA repeat units. It is well-known that the cooperative motion with neighboring segments is necessary for the glass transition.^{53–55} Therefore, the spin-labels move cooperatively with the repeat units of the host polymers in the bulk. As a consequence, it is considered that the motion of the spin-labels reflects the glass transition of the host polymer.

2.2. Influence of Poly(CHMA-random-CHA) Composition on the Mobility of Spin-Labels. The $T_{5.0\text{mT}}$'s of the poly(CHMA-random-CHA)s were plotted as a function of the CHA weight fraction, ϕ_{PCHA} , in Figure 7a. The ESR spectra of the PCHMA, PCHA, and poly(CHMA-random-CHA)s observed at 417 K are shown in Figure 7b. Typically, the ESR spectra of the poly(CHMA-random-CHA) showed a single component. However, the temperature-dependent ESR spectra of the poly(CHMA-random-CHA) with $\phi_{\text{PCHA}} = 0.86$ demonstrated two spectral components. The spectrum comprising two components seemed to be observed at high ϕ_{PCHA} as observed in PCHA homopolymer. Since the

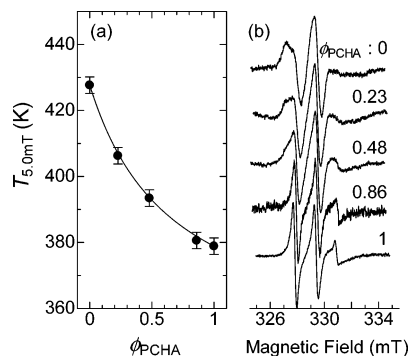


Figure 7. (a) ϕ_{PCHA} -dependent $T_{5.0\text{mT}}$ of poly(CHMA-*random*-CHA). Data are fitted by the Gordon–Taylor equation with $K = 0.4$. (b) ESR spectra of spin-labeled poly(CHMA-*random*-CHA) observed at 417 K.

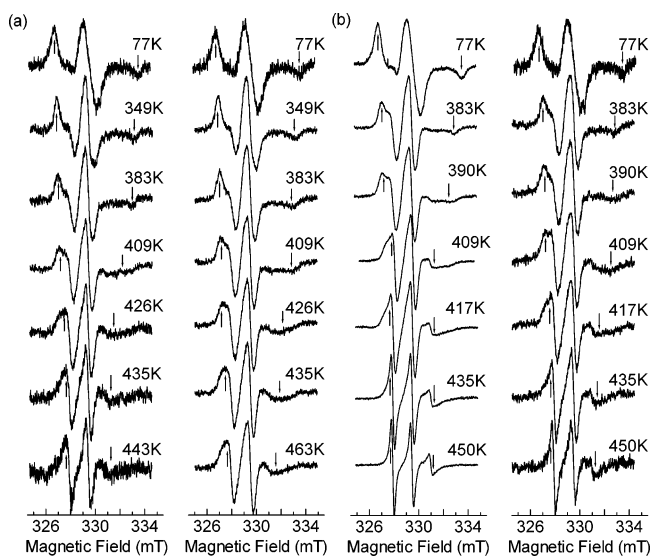


Figure 8. Temperature-dependent ESR spectra of spin-labeled PCHA (left) and PCHMA (right) in the blend with $\phi_{\text{PCHA}} = 0.1$ (a) and 0.5 (b), respectively.

$T_{5.0\text{mT}}$ reflects the glass transition of host polymers, the Gordon–Taylor equation should be reasonable to fit the plots in Figure 7a using the parameter K of 0.4. The composition-dependent $T_{5.0\text{mT}}$ was fitted well with the Gordon–Taylor equation as well as the T_g of the poly(CHMA-*random*-CHA). This is one of the evidences which the $T_{5.0\text{mT}}$ reflects the glass transition of the host polymer. This result demonstrates that the mobility of the spin-label is dependent on the composition around the label. The same behaviors were observed for the spin-labeled poly(styrene-*random*-methyl acrylate) and poly(styrene-*random*-ethyl acrylate) despite the ESR and DSC measurements.⁵

2.3. Segmental Dynamics of the PCHMA and PCHA in the Blend. To estimate the segmental mobilities of the PCHMA and PCHA chains in the blend by the spin-label technique, the “spin-labeled PCHMA”/PCHA and PCHMA/“spin-labeled PCHA” blends which had the same composition were prepared, respectively. Temperature-dependent ESR spectra of the spin-labeled PCHMA and PCHA in the blends ($\phi_{\text{PCHA}} = 0.1$ (a) and 0.5 (b)) were compared in Figure 8. It is interesting that the two spectral components were observed for the temperature-dependent ESR spectra of the PCHA homopolymer (Figure 5), but the ESR spectra of the spin-labeled PCHA in the blends showed a single spectral component. This implies that the dilution of CHA units

around the spin-labels in the blend. Recently, we examined dynamic heterogeneities in the interfacial regions of microphase separations of polystyrene-*block*-poly(methyl acrylate) (PS-*block*-PMA) and polystyrene-*block*-poly(ethyl acrylate) (PS-*block*-PEA) using the ESR spin-label technique.^{5,6} In the previous work, the junction points of the block copolymers were spin-labeled, and the spin-labels were concentrated in the interfacial region of the microphase separations. The mobility of the spin-labels in the interfacial region was almost the mean of those of the both components. In addition, the temperature-dependent ESR spectra of the labels showed two spectral components. We concluded that the two spectral components were brought from a broad distribution of the τ_c induced by the gradient of the segmental concentration in the interfacial region. In the present work, the separated mobilities of the PCHMA and PCHA chains in the blend were observed even in the miscible blend. However, their ESR spectra showed a single spectral component; namely, the dynamic heterogeneity in the PCHMA/PCHA blend is smaller than those in the interfacial regions of the microphase-separated PS-*block*-PMA and PS-*block*-PEA.

The molecular mobilities of the PCHMA and PCHA in the blend with the ϕ_{PCHA} of 0.5 were obviously higher than those in the blend with the ϕ_{PCHA} of 0.1. This result is brought from the depression of the overall T_g of the PCHMA/PCHA blend owing to the increase in the ϕ_{PCHA} . Even though the PCHMA/PCHA blends showed the single glass transitions in the DSC measurements, the different molecular mobilities of the PCHMA and PCHA chains in the blend were detected by the spin-label technique. This is the direct observation of the dynamic heterogeneity in the PCHMA/PCHA blend. The different segmental mobility for each component was detected for another miscible polymer blends.^{13–29} In general, the different segmental mobility for each component has been observed for miscible polymer pairs having a dynamic heterogeneity; i.e., a large difference in their T_g 's and the interaction between the components is weak. For example, the blend systems of polyisoprene/poly(vinylethylene), polystyrene/poly(vinyl methyl ether), polystyrene/poly(phenylene oxide), etc., were reported. As mentioned above, the PCHMA and PCHA also have large difference in the T_g 's (ca. 70 K), and the interaction is considered to be weak with each other (see Figure 2).

The individual motional transition temperatures, $T_{5.0\text{mT}}$'s, of the PCHMA ($T_{5.0\text{mT},\text{PCHMA}}$) and PCHA ($T_{5.0\text{mT},\text{PCHA}}$) chains in the PCHMA/PCHA blend were plotted against the ϕ_{PCHA} in Figure 9. The individual chain dynamics of each component was detected in any compositions. As mentioned above, it is considered that the spin-labels are meshed with neighboring monomeric units in the bulk, and as a result, they move cooperatively with the neighboring units. Therefore, the motion of the spin-labels reflects the segmental mobility around them.^{4,7} As shown in Figure 7, the mobility of the spin-labels is strongly influenced by the composition around the labels.⁵ Thus, we consider that the “effective” compositions around the labels attached to the PCHMA and PCHA chains are different in the blend, and this is the main cause of the different mobilities of the PCHMA and PCHA in the blend.

Leroy et al. showed that the mean segmental dynamics of each component in miscible polymer blends was explained well by the idea of the self-concentration effect proposed by Lodge and McLeish at least for tempera-

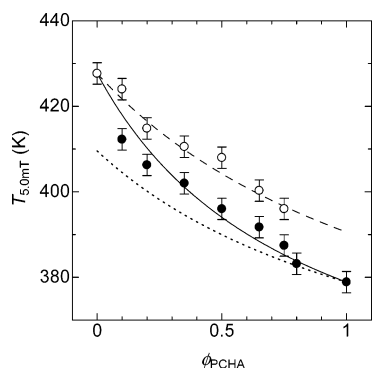


Figure 9. Plots of $T_{5.0mT}$, PCHMA (open) and $T_{5.0mT}$, PCHA (solid) against ϕ_{PCHA} . Broken and dotted curves are $T_{5.0mT, PCHMA}^{eff}$ and $T_{5.0mT, PCHA}^{eff}$ calculated by the Lodge–McLeish model. The solid curve is presented by the Gordon–Taylor equation with $K = 0.4$.

tures above the T_g 's of the components.¹⁶ They bolstered Lodge's idea that the cooperative volume above the glass transition is comparable to the cube of the Kuhn length. Recently, He et al. critically compared literature data for the average segmental or terminal dynamics of components in six different miscible polymer blends to the miscible blend dynamics predicted by the Lodge–McLeish model. They showed that the model successfully fitted the experimental data for a given component with a parameter ϕ_s , which was independent of temperature and composition in most cases.⁵⁶ Kant et al. estimated the temperature dependence on the cooperative volume size in polymer blends from the experimental τ_c data.¹³ They showed that the concentration fluctuation effect on the segmental dynamics became small quickly with an increase in temperature. On the other hand, the temperature dependence of the self-concentration effect brought from the chain connectivity was extremely small. They suggested that the Lodge–McLeish model was reasonable to explain the mean segmental dynamics of each component in the blend at high temperatures.²⁴ However, they proposed that the effect of the concentration fluctuation on the mean segmental dynamics should be considered below the T_g 's of the homopolymers of each component. Anyhow, they concluded that the self-concentration effect provided a good description of the mean segmental dynamics at high temperatures.

The $T_{5.0mT}$ reflects the mean mobility of the spin-labels, and it is ca. 70 K higher than the T_g due to the high frequency of the ESR. Therefore, the effect of the concentration fluctuation on the $T_{5.0mT}$ is considered to be extremely small.^{13,16} The concept of "effective concentration" was first proposed by Chung et al.²⁰ In a miscible polymer blend of polymer A and B, chain connectivity imposes that the local environment of a segment of polymer A is (on average) necessarily richer in polymer A compared to the bulk composition. The effective local concentration sensed by a polymer segment is thus given by

$$\phi_{eff} = \phi_s + (1 - \phi_s)\phi \quad (3)$$

Here, ϕ_s is the "self-concentration" of the considered polymer segment. Lodge and McLeish suggested the way of calculating ϕ_s .²⁴ Their idea is that the length scale relevant to the monomeric friction factor should be of the same order as the Kuhn length, l_k . In their model, it is assumed that the relaxation of the Kuhn

segment is influenced by the concentration of monomers within a volume $V = l_k^3$. The ϕ_s is calculated as the volume fraction occupied by a Kuhn length's worth of monomers inside V :

$$\phi_s = C_\infty M_0 / k\rho N_{av} V \quad (4)$$

where M_0 is the molar mass of the repeat unit, N_{av} is the Avogadro number, k is the number of backbone bonds per repeat unit, ρ is the density, and C_∞ is the characteristic ratio. Lodge and McLeish proposed to calculate the "effective" glass transition temperature, T_g^{eff} , from the effective concentration as

$$T_g^{eff}(\phi) = T_g(\phi)|_{\phi=\phi_{eff}} \quad (5)$$

where $T_g(\phi)$ corresponds to the macroscopic glass transition temperature of the blend of average concentration ϕ . In our case, we assumed the "effective" motional transition temperature, $T_{5.0mT}^{eff}$, as follows:

$$T_{5.0mT}^{eff}(\phi) = T_{5.0mT}(\phi)|_{\phi=\phi_{eff}} \quad (6)$$

We calculated the evolution of the $T_{5.0mT}^{eff}$ of the PCHMA and PCHA following the same procedure as Lodge and McLeish, i.e., by combining eqs 1, 3, and 6. For example, the $T_{5.0mT}^{eff}$ of the PCHA component ($T_{5.0mT, PCHA}^{eff}$) is given by

$$T_{5.0mT, PCHA}^{eff} = (T_{5.0mT, 1}\phi_{eff, PCHA} + KT_{5.0mT, 2}(1 - \phi_{eff, PCHA})) / (\phi_{eff, PCHA} + K(1 - \phi_{eff, PCHA})) \quad (7)$$

where $T_{5.0mT, 1}$ and $T_{5.0mT, 2}$ are the $T_{5.0mT}$ of the PCHA and PCHMA homopolymers, respectively. $\phi_{eff, PCHA}$ is the effective concentration of the PCHA component calculated using eq 3. The self-concentration, ϕ_s , of the PCHMA and PCHA are calculated to be ca. 0.41 and 0.21, respectively.^{57,58}

The $T_{5.0mT, PCHMA}^{eff}$ and $T_{5.0mT, PCHA}^{eff}$ predicted by the Lodge–McLeish model were presented as broken and dotted lines in Figure 9, respectively. Here, the K in eq 7 is substituted to be 0.4. The predicted $T_{5.0mT, PCHMA}^{eff}$ is in excellent agreement with the experimental $T_{5.0mT, PCHMA}$. This agreement implies that the scale of the region explored by the label is comparable to the control volume size, $V = l_k^3$, suggested by Lodge and McLeish when it is assumed that the mobility of the spin-labels is controlled by only "effective" composition around the labels. Previously, the cooperative volume of PMMA explored by the spin-labels was estimated to be ca. 1.0 nm³.⁷ On the other hand, the V of the PMMA by the Lodge–McLeish assumption is calculated to be ca. 2.6 nm³.²⁴ We consider that these values are almost comparable with each other.

The Lodge–McLeish model qualitatively captured the feature of the $T_{5.0mT, PCHA}$. However, the experimental $T_{5.0mT, PCHA}$ was slightly higher than the $T_{5.0mT, PCHA}^{eff}$ predicted by the Lodge–McLeish model. One of the causes of this slight disagreement may be related to the approximate parameters used to calculate the ϕ_s and the simplification of the Lodge–McLeish model. The motion of the nitroxides labeled to the PCHA might be restricted by the rigid PCHMA component in the blend although the cause of this manner is unknown. Using the ESR spin-label technique, the mobility of mobile poly(acrylate)s in multicomponents systems is often

estimated to be somewhat lower than expected one. In our previous paper, segmental dynamics of both components in microphase separation of PS-*block*-PMA was estimated by the spin-label technique and DSC.⁵ The T_g 's of the PS and PMA components in the PS-*block*-PMA were comparable to those of PS and PMA homopolymers, respectively, and the $T_{5,0mT}$ of the PS component in the PS-*block*-PMA was almost same with that of the PS homopolymer. On the other hand, the $T_{5,0mT}$ of the PMA component was obviously higher than that of the PMA homopolymer. This result concluded that the mobility of the PMA chain was strongly restricted by the rigid PS component. This can be thought of the similar behavior of spin-labeled PCHA in this study. The understanding for this feature detected by the spin-label technique is of essential importance; however, it is still difficult because of the lack of study on mobility of spin-labeled polyacrylates.

Conclusion

The different segmental dynamics of the PCHMA and PCHA chains in the blend were detected by the spin-label technique even though the thermodynamically miscible blend was indicated by the DSC measurement. The $T_{5,0mT}$ showed the similar composition dependence of the poly(CHMA-*random*-CHA) with the T_g . This indicated that the mobility of the spin-label was sensitive to the composition around the label. The $T_{5,0mT}$ was ca. 70 K higher than the T_g because of the high frequency of the ESR. The self-concentration model suggested by Lodge and McLeish was available for prediction of the mean segmental mobility of the PCHMA and PCHA chains in the blend detected by the spin-label. The Lodge–McLeish model provided the qualitative feature for the $T_{5,0mT,PCHA}$ although the experimental values were slightly higher than the calculated ones. On the other hand, the $T_{5,0mT,PCHMA}^{eff}$ predicted by the Lodge–McLeish model quantitatively agreed with the experimental $T_{5,0mT,PCHMA}$. These results implied that the region explored by the spin-label was comparable to the control volume $V = l_k^3$. This result was supported by our previous work about the size of the cooperative volume in PMMA estimated by the ESR method. As a conclusion, the specific segmental dynamics of the PCHMA and PCHA in the blend was detected by the ESR spin-label technique. The motion of the spin-labels sensitively reflected the local dynamic environment around them.

Acknowledgment. This research was partially supported by the Ministry of Education, Science, Sports and Culture, Grant-in-Aid for Young Scientists (B), 16750185, 2004. Thanks are due to the Research Center for Molecular-Scale Nanoscience, the Institute for Molecular Science, for assistance in obtaining the DSC data. The financial support of a part of this project is by a grant from the NITECH 21st Century COE Program "World Ceramics Center for Environmental Harmony".

References and Notes

- (1) Faetti, M.; Giordano, D.; Leporini, D.; Pardi, L. *Macromolecules* **1999**, *32*, 1876.
- (2) Schlick, S.; Harvey, R. D.; Alonso-Amigo, M. G.; Klempner, D. *Macromolecules* **1989**, *22*, 822.
- (3) Müller, G.; Stadler, R.; Schlick, S. *Macromolecules* **1994**, *27*, 1555.
- (4) Miwa, Y.; Tanase, T.; Yamamoto, K.; Sakaguchi, M.; Sakai, M.; Shimada, S. *Macromolecules* **2003**, *36*, 3235.
- (5) Miwa, Y.; Yamamoto, K.; Sakaguchi, M.; Sakai, M.; Tanida, K.; Hara, S.; Okamoto, S.; Shimada, S. *Macromolecules* **2004**, *37*, 831.
- (6) Miwa, Y.; Tanida, K.; Yamamoto, K.; Okamoto, S.; Sakaguchi, M.; Sakai, M.; Makita, S.; Sakurai, S.; Shimada, S. *Macromolecules* **2004**, *37*, 3707.
- (7) Miwa, Y.; Yamamoto, K.; Sakaguchi, M.; Sakai, M.; Makita, S.; Shimada, S. *J. Phys. Chem.*, to be submitted.
- (8) Brown, I. M.; Sandreczki, T. C. *Macromolecules* **1985**, *18*, 2702.
- (9) Sakaguchi, M.; Shimada, S.; Yamamoto, K.; Sakai, M. *Macromolecules* **1997**, *30*, 3629.
- (10) Yamamoto, K.; Shimada, S.; Ohira, K.; Sakaguchi, M.; Tsujita, Y. *Macromolecules* **1997**, *30*, 6575.
- (11) Shimada, S.; Hane, Y.; Watanabe, T. *Polymer* **1997**, *38*, 4667.
- (12) Cameron, G. G.; Qureshi, M. Y.; Ross, E.; Miles, I. S.; Richardson, J. *Eur. Polym. J.* **1991**, *27*, 1181.
- (13) Kant, R.; Kumar, S. K.; Colby, R. H. *Macromolecules* **2003**, *36*, 10087.
- (14) Salaniwai, S.; Kant, R.; Colby, R. H.; Kumar, S. K. *Macromolecules* **2002**, *35*, 9211.
- (15) Kumar, S. K.; Colby, R. H.; Anastasiadis, S. H.; fytas, G. *J. Chem. Phys.* **1996**, *105*, 377.
- (16) Leroy, E.; Alegria, A.; Colmenero, J. *Macromolecules* **2003**, *36*, 7280.
- (17) Leroy, E.; Alegria, A.; Colmenero, J. *Macromolecules* **2002**, *35*, 5587.
- (18) Colby, R. H. *Polymer* **1989**, *30*, 1275.
- (19) Chung, G.-C.; Kornfield, J. A.; Smith, S. D. *Macromolecules* **1994**, *27*, 964.
- (20) Chung, G.-C.; Kornfield, J. A.; Smith, S. D. *Macromolecules* **1994**, *27*, 5729.
- (21) Alegria, A.; Colmenero, J.; Ngai, K. L.; Roland, C. M. *Macromolecules* **1994**, *27*, 4486.
- (22) Alvarez, F.; Alegria, A.; Colmenero, J. *Macromolecules* **1997**, *30*, 597.
- (23) Cendoya, I. M.; Alegria, A.; Colmenero, J.; Grimm, H.; Richter, D.; Frick, B. *Macromolecules* **1999**, *32*, 4065.
- (24) Lodge, T. P.; McLeish, T. C. B. *Macromolecules* **2000**, *33*, 5278.
- (25) Yang, X.; Halasa, A.; Hsu, W. L.; Wang, S. Q. *Macromolecules* **2001**, *34*, 8532.
- (26) Roland, C. M.; Ngai, K. L. *Prog. Colloid Polym. Sci.* **1993**, *91*, 75.
- (27) Min, B.; Qiu, X.; Ediger, M. D.; Pitsikalis, M.; Hadjichristidis, N. *Macromolecules* **2001**, *34*, 4466.
- (28) Zetsche, A.; Fischer, E. W. *Acta Polym.* **1994**, *45*, 168.
- (29) Kamath, S.; Colby, R. H.; Kumar, S. K.; Karatasos, K.; Floudas, G.; Fytas, G.; Roovers, J. E. L. *J. Chem. Phys.* **1999**, *111*, 6121.
- (30) Haley, C. J.; Lodge, P. T.; He, Y.; Ediger, M. D.; von Meerwall, E. D.; Mijovic, J. *Macromolecules* **2003**, *36*, 6142.
- (31) Alegria, A.; Gomez, D.; Colmenero, J. *Macromolecules* **2002**, *35*, 2030.
- (32) Hoffmann, S.; Willner, L.; Richter, D.; Arbe, A.; Colmenero, J.; Farago, B. *Phys. Rev. Lett.* **2000**, *85*, 772.
- (33) Müller, G.; Stadler, R.; Schlick, S. *Macromolecules* **1994**, *27*, 1555.
- (34) Shimada, S.; Hori, Y.; Kashiwabara, H. *Macromolecules* **1988**, *21*, 2107.
- (35) Siol, W.; GmbH, R. *Makromol. Chem., Macromol. Symp.* **1991**, *44*, 47.
- (36) Gordon, M.; Taylor, S. J. *J. Appl. Chem.* **1952**, *2*, 4.
- (37) Kim, E.; Kramer, E. J.; Wu, W. C.; Garrett, P. D. *Polymer* **1994**, *35*, 5706.
- (38) Schneider, H. A. *J. Therm. Anal. Calorim.* **1999**, *56*, 983.
- (39) Cameron, G. G.; Qureshi, M. Y.; Tavern, S. C. *Eur. Polym. J.* **1996**, *32*, 587.
- (40) Brown, I. M. *Macromolecules* **1981**, *14*, 801.
- (41) Shimada, S.; Kozakai, M.; Yamamoto, K. *Polymer* **1998**, *39*, 6013.
- (42) Varghese, B.; Schlick, S. *J. Polym. Sci., Part B: Polym. Phys.* **2002**, *40*, 415.
- (43) Cameron, G. G.; Qureshi, M. Y.; Stewart, D.; Buscall, R.; Nemcek, J. *Polymer* **1995**, *36*, 3071.
- (44) Cameron, G. G.; Stewart, D. *Polymer* **1996**, *37*, 5329.
- (45) Cameron, G. G.; Miles, I. S.; Bullock, A. T. *Br. Polym. J.* **1987**, *19*, 129.
- (46) Shimada, S.; Kashima, K. *Polym. J.* **1996**, *28*, 690.
- (47) Sohma, J.; Sakaguchi, M. *Adv. Polym. Sci.* **1978**, *20*, 109.

- (48) Kusumoto, N.; Sano, S.; Zaitse, N.; Motozato, Y. *Polymer* **1976**, *17*, 448.
- (49) Williams, M. L.; Landel, R. F.; Ferry, J. D. *J. Am. Chem. Soc.* **1995**, *77*, 3701.
- (50) Törmälä, P.; Weber, G. *Polymer* **1978**, *19*, 1026.
- (51) Angell, C. A. *J. Non-Cryst. Solids* **1991**, *131–133*, 13.
- (52) Ngai, K. L.; Plazek, D. J. *Rubber Chem. Technol.* **1995**, *68*, 376.
- (53) Matsuoka, S.; Quan, X. *Macromolecules* **1991**, *24*, 2770.
- (54) Donth, E. *J. Non-Cryst. Solids* **1982**, *53*, 325.
- (55) Kanaya, T.; Tsukushi, T.; Kaji, K.; Bartos, J.; Kristiak, J. *Phys. Rev.* **1999**, *60*, 1906.
- (56) He, Y.; Lutz, T. R.; Ediger, M. D. *J. Chem. Phys.* **2003**, *119*, 9956.
- (57) ϕ_s of PCHMA was calculated from eq 4, using $M_0 = 168.24$ g/mol, $\rho = 1.10$ g/cm³ (Hoff, E. A. W.; Robinson, D. W.; Willbourn, A. H. *J. Polym. Sci.* **1955**, *18*, 161), and $k = 2$. C_∞ and l_k were 9.25 and 14.2 Å, respectively (*Polymer Handbook*, 3rd ed.; John Wiley & Sons: New York, 1989).
- (58) ϕ_s of PCHA was calculated using $M_0 = 154.21$ g/mol, $\rho = 1.10$ g/cm³ (Shao, H. H.; Rabeony, M.; Liang, K. S.; Siakali-Kioulala, E.; Hadjichristidis, N. *Composites, Part A* **1998**, *2*, 113), and $k = 2$. C_∞ was calculated from the radius of gyration at the θ state and the degree of polymerization (Mathakiya, I.; Rakshit, A. K.; Rao, P. V. C. *Int. J. Polym. Anal. Charact.* **2003**, *8*, 339). The C_∞ and l_k were 12.2 and 18.7 Å, respectively.

MA049026R